

Optics Letters

On-chip two-step microwave frequency measurement with high accuracy and ultra-wide bandwidth using add-drop micro-disk resonators

YANG CHEN,^{1,2,*} WEIFENG ZHANG,² JINGXUAN LIU,² AND JIANPING YAO²

¹Shanghai Key Laboratory of Multidimensional Information Processing, East China Normal University, Shanghai 200241, China

²Microwave Photonics Research Laboratory, School of Electrical Engineering and Computer Science, University of Ottawa, 800 King Edward Avenue, Ottawa, Ontario K1N 6N5, Canada

*Corresponding author: ychen@ce.ecnu.edu.cn

Received 14 March 2019; revised 10 April 2019; accepted 11 April 2019; posted 12 April 2019 (Doc. ID 362344); published 6 May 2019

An on-chip two-step microwave frequency measurement method with high accuracy and an ultra-wide frequency measurement range is reported. A silicon photonic integrated micro-disk resonator (MDR) array is used to coarsely measure the signal frequency via an array of add-drop MDRs with smaller disk radii; then an MDR with a larger radius is used to finely measure the signal frequency, which is done by monitoring the optical powers of the optical signals from the through port and drop port of the MDRs. The proposed system features a very compact structure, ultra-wide frequency measurement range, and high frequency measurement accuracy, which is verified by a proof-of-concept experiment using two MDRs with radii of 6 and 10 μm . A frequency measurement of microwave signals from 1.6 to 40 GHz is implemented with a measurement error of less than 60 MHz. The stability of the system is also evaluated. © 2019 Optical Society of America

<https://doi.org/10.1364/OL.44.002402>

In modern radar warning and electronic warfare systems, it is highly desirable that the frequency of an unknown microwave signal can be finely measured [1]. With the rapid development of electronic systems, the frequency of a microwave signal can be very high and largely tunable; therefore, a frequency measurement system that can perform a microwave frequency measurement (MFM) up to tens or even hundreds of gigahertz is needed, while high measurement accuracy is still required. Conventional electronic techniques cannot fulfill these requirements. Microwave photonics that can support high frequency and wideband operation is considered a solution to implement ultra-wideband MFM [2,3].

The commonly used photonic method to implement MFM is to map the frequency of an unknown microwave signal to an amplitude comparison function (ACF). The ACF can be obtained by using a polarization-maintaining fiber-based [4,5] or a dispersive medium-based [6–8] filter. The disadvantage of this method is that the size of the systems is large, especially

when a long fiber is needed, which makes it hard to integrate the systems. To reduce the size, on-chip solutions have been proposed. In Refs. [9,10], an ACF is built using a micro-disk resonator (MDR) or a micro-ring resonator. In Ref. [11], the nonlinear effect in an optomechanical micro-ring resonator is utilized to establish an ACF. However, the methods in Refs. [9–11] cannot fulfill the needs of ultra-wideband MFM, because the MFM range is limited by the bandwidth of the resonance notch of the resonators. In addition, the ACFs in Refs. [9–11] are constructed by monitoring the electrical powers after the unknown signal is filtered by a microwave photonic filter, so a pair of photodetectors is needed, which makes the system complicated and costly.

In this Letter, we propose and experimentally demonstrate an approach to achieve MFM with high accuracy and an ultra-wide frequency measurement range. In the proposed system, an array of silicon photonic integrated MDRs with smaller disk radii is used to coarsely measure the signal frequency; then an MDR with a larger radius is used to finely measure the signal frequency, which is done by monitoring the optical powers of the optical signals from the through port and drop port of the MDRs. A proof-of-concept experiment is performed, in which two MDRs with one having a small radius of 6 μm and the other with a large radius of 10 μm are used to achieve coarse and fine frequency measurements, respectively. A frequency measurement range from 1.6 to 40 GHz and a measurement error of less than 60 MHz are demonstrated.

Before we start to discuss our proposed multiple-MDR-based MFM, we begin with a discussion on MFM using a single MDR. Figure 1 shows the schematic diagram of an MFM system based on a single add-drop MDR. A carrier-suppressed single-sideband (CS-SSB) optical signal that is generated by modulating an optical carrier with an unknown microwave signal is sent to an MDR with the optical carrier located outside the notch of the spectral response. Depending on the location of the optical carrier, the sideband falls into the resonance notch at different frequencies. As shown in Fig. 1, f_1 is the frequency at the edge of the flat response, f_2 is the frequency at the center of the notch, and the frequency difference between these two

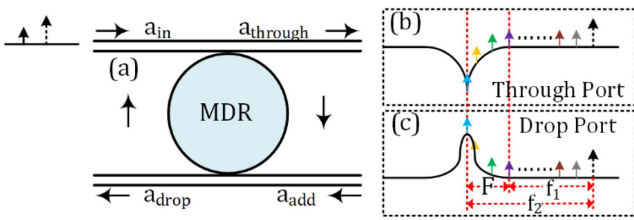


Fig. 1. Schematic diagram of an MFM system based on a single MDR.

frequencies is noted as F . Since a monotonically increasing ACF between f_1 and f_2 can be constructed by comparing the optical powers from the through port and drop port, the frequency of the unknown microwave signal can be measured using the ACF. By adjusting the location of the optical carrier, the MFM range can be accordingly shifted.

The concept using a single MDR for MFM shown in Fig. 1 can be extended to have multiple MDRs for MFM with an improved accuracy and measurement range. Figure 2(a) shows the schematic of the proposed two-step MFM system using an array of add-drop MDRs with smaller disk radii and an MDR with a larger radius. An optical frequency comb is CS-SSB modulated by an unknown microwave signal, and then sent to an array of N MDRs having a smaller and identical radius r_1 via an arrayed waveguide grating (AWG). The optical carriers have a fixed wavelength relationship with the N different notches from the N MDRs, as shown in Fig. 2(b), and the AWG filters out the optical wavelengths outside the ranges of

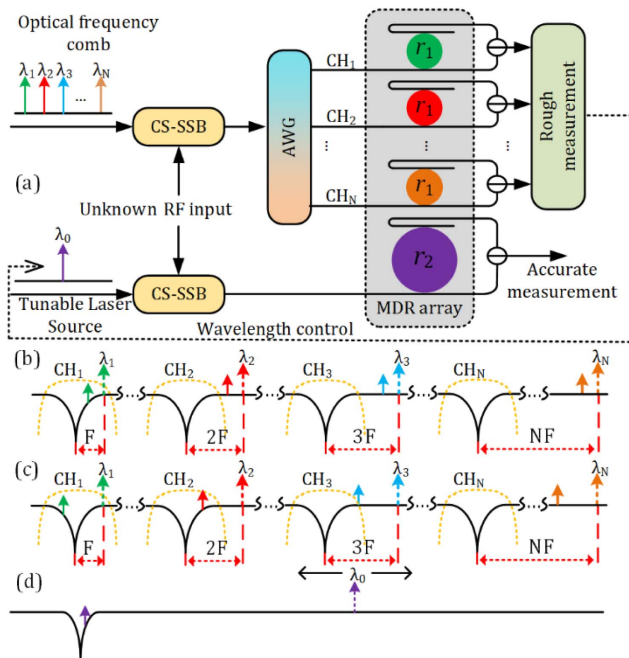


Fig. 2. Schematic diagrams of (a) an on-chip two-step MFM system based on an array of small radius add-drop MDRs and a single large radius MDR; (b) the locations of the optical carriers and sidebands with a low frequency microwave signal; (c) the locations of the optical carriers and sidebands with a high frequency microwave signal; and (d) the locations of the optical carrier and sideband for fine measurement.

the N different notches. When the frequency of the unknown microwave signal is low, only the optical sideband of the optical carrier nearest the notches (λ_1) falls into the right side of the notch. After comparing the powers at the through ports and drop ports of the N MDRs, the frequency of the microwave signal can be coarsely identified. If the frequency of the microwave signal is higher than the frequency spacing F , as shown in Fig. 2(c), the optical sideband of the carrier λ_2 falls into the right side of the notch, whereas the optical sideband of the carrier λ_1 falls into the left side of the notch. It is clear that the results from the ACF of the first MDR are incorrect, so we only calculate the frequency of the microwave signal according to the ACF of the second MDR. Since the frequency spacing of the wavelengths are well designed, no matter how high the frequency of the microwave signal is, only two sidebands of two adjacent carriers fall into the notches. We can determine the frequency of the microwave signal according to the ACF of the MDR with a sideband on the right side of its notch.

A second path, starting with a tunable laser source (TLS), is used for a fine frequency measurement. The lightwave from the TLS is also CS-SSB modulated by the same unknown microwave signal. The CS-SSB modulated optical signal is sent to the MDR with a larger radius r_2 , whose transmission notch is much narrower than that of the MDRs with radius r_1 . After getting the coarse frequency of the unknown signal, the optical carrier from the TLS is fast tuned to make the optical sideband of the microwave carrier fall into the sharp right side of the notch. The optical power ratio between the through port and drop port of the MDR will give a finer frequency measurement of the microwave signal.

A proof-of-concept experiment is carried out based on the setup shown in Fig. 3(a). An optical carrier from a TLS (Anritsu, MG9638A) is injected into a Mach-Zehnder modulator (MZM, Optilab IM-1550-40-PM), where the optical carrier is carrier-suppressed double-sideband modulated (CS-DSB) by a microwave signal from a microwave signal generator (MSG, Agilent E8254A). Then an optical waveshaper (OWS, Finisar Waveshaper 4000S) is used to remove the lower optical sideband to get only a single sideband. The single-sideband optical signal is then sent to an add-drop MDR with two output ports. The powers at the through port and the drop port of the MDR are measured using an optical average power meter (OAPM, HP 8152A). The power ratio between the two optical signals from the two output ports corresponding to the ACF is

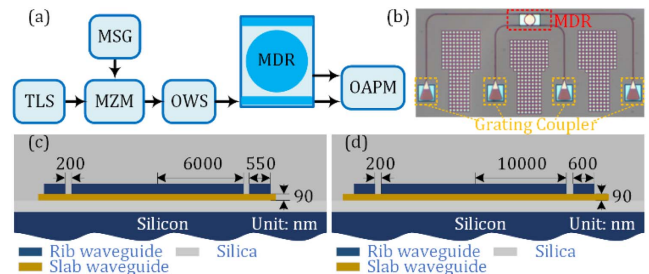


Fig. 3. (a) Experimental setup of the on-chip two-step MFM method. TLS, tunable laser source; MSG, microwave signal generator; MZM, Mach-Zehner modulator; OWS, optical waveshaper; and OAPM, optical average power meter. (b) Schematic layout of the designed on-chip add-drop MDR with a 10- μm radius. Cross-sectional view of the add-drop MDRs with radii of (c) 6 and (d) 10 μm .

calculated to estimate the frequency of the input microwave signal. Figure 3(b) presents the schematic layout of an on-chip add-drop MDR with a 10- μm radius. Figures 3(c) and 3(d) show the cross-sectional views of the two MDRs used in the experiment, which have radii of 6 and 10 μm , respectively.

First, the spectral responses of the two MDRs used in the experiment are measured by an optical vector analyzer (LUNA, OVA 5000). Figures 4(a) and 4(b) show the spectral responses of the 6- μm MDR, when the output is taken from the through port and drop port, respectively. Multiple resonance notches and peaks are observed. The zoom-in views of the first resonance notch and peak outlined in the dotted boxes are shown in Figs. 4(c) and 4(d). The 3 dB bandwidth of the notch is about 165.68 pm, or 21.17 GHz. Figure 5 shows the spectrum response of the 10 μm MDR. The 3-dB bandwidth of the third notch is about 35.53 pm, which equals 4.50 GHz. Since the bandwidth of the notch in the 10- μm MDR is much smaller compared with that in the 6- μm MDR, a finer measurement can be achieved. In comparison, the 6- μm MDR has a much wider frequency measurement range.

Then we use the 6- μm MDR to achieve a wideband coarse frequency measurement. The TLS is tuned to make the frequency spacing between the first notch of the 6- μm MDR and the optical carrier to be 22.2 GHz. It is shown in Fig. 6(a) that one sideband of the CS-DSB signal from the MZM is filtered out by the OWS, and a single-sideband

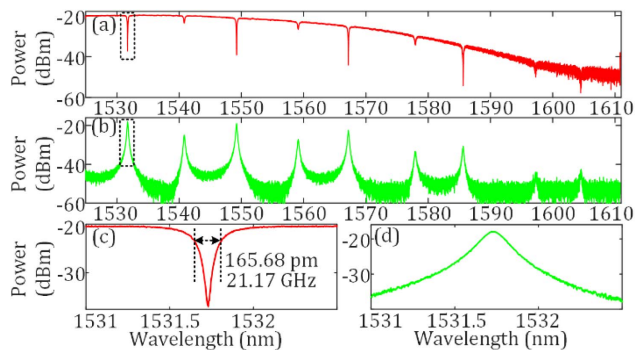


Fig. 4. Spectral responses of the 6- μm MDR from the (a) through port and (b) drop port. Zoom-in views of the (c) notch and (d) peak at 1531.73 nm in the dotted boxes in (a) and (b).

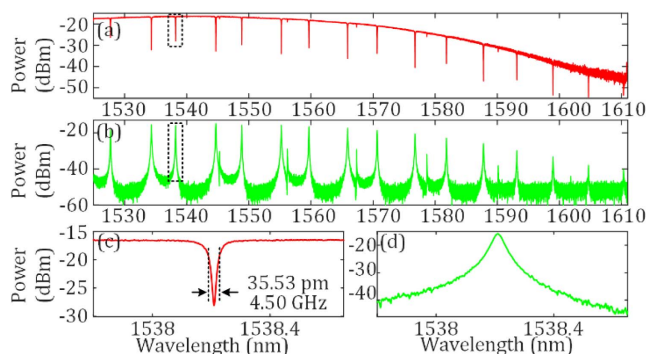


Fig. 5. Spectral responses of the 10- μm MDR from the (a) through port and (b) drop port. Zoom-in views of the (c) notch and (d) peak at 1538.21 nm in the dotted boxes in (a) and (b).

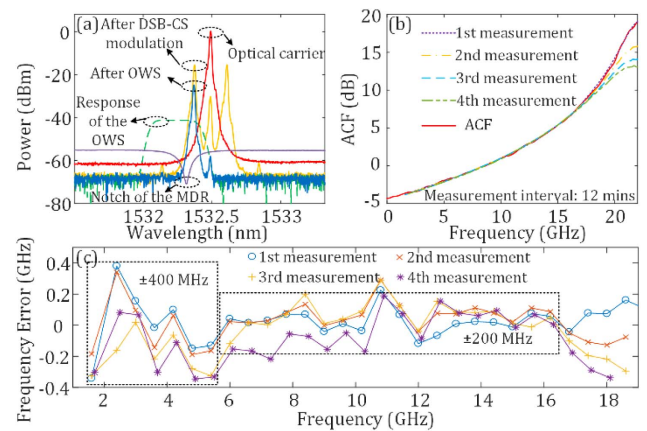


Fig. 6. (a) Single-sideband signal generation, (b) ACF from the measurement results in Figs. 4(c) and 4(d), and four measured ACFs, and (c) measurement errors in the range from 1.6 to 18.6 GHz.

optical signal is generated. Figure 6(b) shows the theoretical ACF from the responses shown in Figs. 4(c) and 4(d), and four measured ACFs. From 1.6 to 18 GHz, the measured ACFs show good agreement with the theoretical ACF. When the signal frequency is higher than 18 GHz, the measured ACFs have a large difference from the theoretical ACF. This is caused by the small wavelength drift of the TLS. Since the notch is nearly 20 dB in depth, a small wavelength drift will cause a significant power variation from the through port when the optical sideband is near the center of the notch. Figure 6(c) shows the measurement errors of four measurements in the frequency range from 1.6 to 18 GHz. The errors in the range from 6 to 16.2 GHz are about ± 200 MHz. When the frequency is lower than 6 GHz, the measurement errors are about ± 400 MHz. The measurement errors are worse than ± 200 MHz when the frequency is higher than 16.2 GHz.

Then the wavelength of the TLS is tuned to be 41.2 GHz away from the notch of the 6- μm MDR to evaluate the frequency measurement in a higher frequency band. The generation of a single-sideband signal is shown in Fig. 7(a). Figure 7(b) shows the theoretical ACF from the responses shown in Figs. 4(c) and 4(d), and four measured ACFs. The measurement errors are shown in Fig. 7(c). The errors in the first three measurements are limited to ± 200 MHz in the frequency range from 24.8 to 34.4 GHz. When the frequency is outside this range, the upper bound of the errors increases to about +300 MHz. Specifically, it is noticed that the error of the fourth measurement is larger than those of the first three measurements, which is due to a larger wavelength drift of the optical carrier caused by the long-term operation of the TLS. In Fig. 6(c), this phenomenon is also observed.

Finally, a fine frequency measurement is implemented using the 10- μm add-drop MDR. Figure 8 shows the errors of the measured frequency in four different frequency bands. For the measurement in Fig. 8(a), it is found that a fine measurement with errors less than ± 50 MHz is achieved in a 4.8 GHz frequency range from 4 to 8.8 GHz, in the first three measurements. Figure 8(b) shows the measurement errors in the frequency range from 13 to 19 GHz. The measurement errors are also less than ± 50 MHz in the first three measurements in a frequency band of 4.4 GHz. The fourth

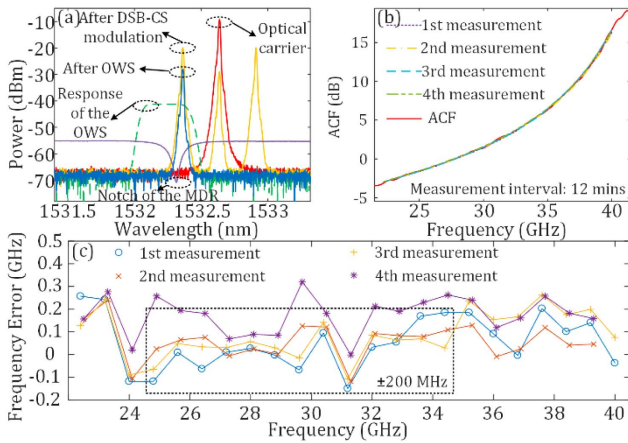


Fig. 7. (a) Single-sideband signal generation, (b) ACF from the measurement results in Figs. 4(c) and 4(d), and four measured ACFs, and (c) measurement errors in the range from 22.4 to 40 GHz.

measurements in Figs. 8(a) and 8(b) have relatively larger errors due to the wavelength drift of the TLS in long-term operation. Figures 8(c) and 8(d) show the measurement errors in two frequency ranges from 23 to 29 GHz and from 32 to 38.6 GHz, which can reach measurement accuracies of ± 60 MHz in a 5.2 GHz frequency range and ± 45 MHz in a 4.4 GHz frequency range, respectively, in the first two measurements. The measurement accuracies of the third measurements in

these two cases deteriorate slightly, whereas those of the fourth measurements have much larger errors up to 200 and -150 MHz, respectively. If the system for fine measurement is in free running for a relatively longer time, the accuracy of the measurement decreases much faster than that of the coarse measurement. The reason is that the resonance notch used in the fine measurement is much narrower than that used in the coarse measurement, so the system is more sensitive to the environment changes and wavelength drift of the TLS.

Regarding the real-time performance of the MFM, the first step is implemented in real time, and the second step takes a little more time, mainly depending on the tuning speed of the TLS. The measurement range can be further increased by using more optical carriers and an MDR array, as shown in Fig. 2, and the accuracy of the measurement can be increased by using an MDR with a larger radius. In the case shown in Fig. 2, an integrated CS-SSB modulator is a better choice compared with an MZM plus an OWS. The stability of the system, which was mainly limited by the wavelength stability of the TLS ($< \pm 100$ MHz/h in the experiment), was evaluated, and four measurements in 48 min were performed. Good stability within 24 min was achieved. If the system was free running longer than 36 min, a calibration of the ACF curve using some known frequencies was needed to maintain high measurement accuracy. In addition, the proposed system in Fig. 2 can also be used to measure signals with multiple frequencies. The frequencies of the signals can be determined in many equally spaced frequency ranges that are equal to the bandwidth of the resonance notches of the MDRs. We can use MDRs with narrower notches, so that the frequencies of the multiple microwave signals can be determined in smaller frequency ranges. Since the optical sidebands of some frequencies may fall into the same notch, further measurements in a small frequency range are needed to identify each frequency.

Funding. Natural Sciences and Engineering Research Council of Canada (NSERC); National Natural Science Foundation of China (NSFC) (61601297); Open Fund of IPOC (BUPT).

REFERENCES

1. D. C. Schleher, *Electronic Warfare in the Information Age* (Artech House, 1999).
2. X. Zou, B. Lu, W. Pan, L. Yan, A. Stöhr, and J. Yao, *Laser Photonics Rev.* **10**, 711 (2016).
3. J. Yao, *J. Lightwave Technol.* **27**, 314 (2009).
4. X. Zou, H. Chi, and J. Yao, *IEEE Trans. Microw. Theory Tech.* **57**, 505 (2009).
5. S. Pan and J. Yao, *IEEE Photonics Technol. Lett.* **22**, 1437 (2010).
6. M. Attygalle and D. B. Hunter, *IEEE Photonics Technol. Lett.* **21**, 206 (2009).
7. L. V. T. Nguyen and D. B. Hunter, *IEEE Photonics Technol. Lett.* **18**, 1188 (2006).
8. Y. Zhao, X. Pang, L. Deng, X. Yu, X. Zheng, B. Zhou, and I. T. Monroy, *Opt. Express* **19**, B681 (2011).
9. L. Liu, F. Jiang, S. Yan, S. Min, M. He, D. Gao, and J. Dong, *Opt. Commun.* **335**, 266 (2015).
10. J. Jiang, H. Shao, X. Li, Y. Li, T. Dai, G. Wang, J. Yang, X. Jiang, and H. Yu, *Opt. Commun.* **382**, 366 (2017).
11. L. Liu, H. Qiu, Z. Chen, and Z. Yu, *IEEE Photonics J.* **9**, 5503611 (2017).

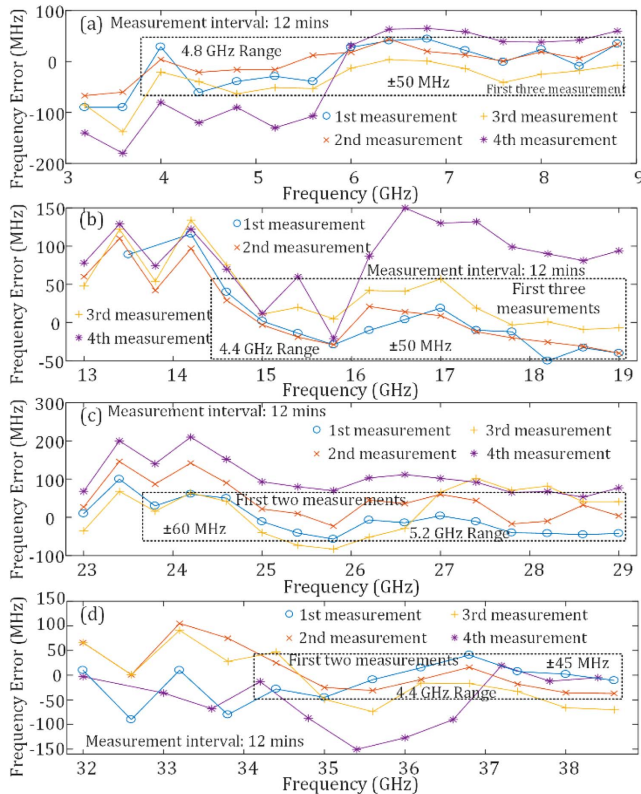


Fig. 8. Measurement errors in the range (a) from 3.2 to 8.8 GHz, (b) from 13 to 19 GHz, (c) from 23 to 29 GHz, and (d) from 32 to 38.6 GHz.